Int. J. Electrochem. Sci., 14 **(2019)** 11048 – 11056, doi: 10.20964/2019.12.64

International Journal of
ELECTROCHEMICAL
SCIENCE
www.electrochemsci.org

Short Communication

Hollow $NiCo_2O_4$ Nanofibers Prepared by Electrospinning as an Effective Sulfur Host for High-Performance Lithium-Sulfur Batteries

Bin Cai, Yuning Meng[*], *MengEn Zhu, Peng Peng*

Department of Chemistry & Chemical Engineering, Zhoukou Normal University, Zhoukou, 466001, Henan, P. R. China
[*]E-mail: ynmeng@aliyun.com

Received: 15 July 2019 / *Accepted:* 26 September 2019 / *Published:* 29 October 2019

Many achievements have been obtained for the lithium-sulfur battery by using various superior host materials for the element sulfur. However, the sulfur loading in the previous works is under 2 mg cm^{-2}. As we all know, the high energy density could be improved only when the sulfur loading exceeds 3 mg cm^{-2}. Therefore, it is urgent for the researchers to develop high-loading sulfur electrode materials for the lithium-sulfur batteries. In our work, the hollow $NiCo_2O_4$ nanofibers are prepared and used host materials for the sulfur. The sulfur loading of the as-prepared S/$NiCo_2O_4$ electrode is 4 mg cm^{-2} with superior cycle stability.

Keywords: High-loading electrode, Li-S battery, Cycle performance, Specific capacity

1. INTRODUCTION

In the past decades, many researchers have devoted themselves to the research of the lithium-sulfur batteries [1, 2]. The lithium-sulfur batteries have high specific capacity (1675 mAh g^{-1}) and energy density (2600 Wh Kg^{-1}) [3, 4, 5]. Moreover, the element sulfur is abundant and no pollution for the environment [6, 7]. Therefore, the lithium-sulfur battery could be the most promising energy storage system for the electric vehicles [8, 9]. However, there are also some disadvantages: a) the poor electronic conductivity of the element sulfur; b) the severe shuttle effect of the soluble polysulfide [10, 11].

So far, many strategies have been applied to solve these problems, including especially, the design of the perfect host materials for the element sulfur [12]. Few studies are focusing on the sulfur loading of the lithium-sulfur battery [13]. The sulfur loading has direct influence on the energy density of the lithium-sulfur battery. But the sulfur loadings in the previous works were mostly under 2 mg cm^{-}

^{2} [14]. Consequently, the researchers begin to develop the high-loading sulfur electrode. Peng et al used graphitized porous carbon as host materials for the sulfur to prepare high-loading lithium-sulfur battery with 4 mg cm^{-2} [15].

In our work, the hollow $NiCo_2O_4$ nanofibers were prepared and used as the host materials for the sulfur. The as-prepared $S/NiCo_2O_4$ electrode with high-loading sulfur shows excellent electrochemical performance. The initial specific capacity of the $S/NiCo_2O_4$ electrode is as high as 1096 mAh g-1 at 0.2 C. Even at 1 C, the specific capacity is as high as 835 mAh g^{-1} with high-loading sulfur of 4 mg cm^{-2}.

2. EXPERIMENTAL

2.1 Preparation of $NiCo_2O_4$ nanofiber

First, 1.5 mol $Co(CH_3COO)_2{\cdot}4H_2O$, 0.75 mol $Ni(CH_3COO)_2{\cdot}4H_2O$ and 0.7 g PAN were dissolved into 20 ml N,N-dimethylformamide to prepare precursor solution. After that, the pure $NiCo_2O_4$ nanofibers were synthesized via electrospinning method
with a flow rate of 2 mL h^{-1}. And the distance and voltage between the nozzle and collector were 12 cm and 15 kV, respectively [16]. Finally, the hollow nanofbers were prepared by calcination at 500 °C for 2 h.

2.2 Preparation of $S/NiCo_2O_4$ composites

The $S/NiCo_2O_4$ composites were prepared by using heating method at the temperature of 155℃ for 12 h in the N_2 atmosphere. After cooling to the room temperature, the prepared product was ground for 30 min. As a result, the $S/NiCo_2O_4$ composites were successfully obtained.

2.2 Materials Characterization

The morphologies of the samples were observed by using scanning electronic microscope (SEM, Ultra). The crystal structure of the sample was tested by using X-ray diffraction (XRD). The chemical valance of the composites was tested by using X-ray photoelectron spectroscopy (XPS).

2.3 Electrochemical Tests

The electrochemical performance of the samples was tested by using coin 2032 half battery. Typically, the electrode slurry was prepared by mixing active materials, carbon black and PVDF with a ratio of 88:2:10. NMP was used as solvent. Next, the prepared electrode slurry was uniformly coated on the surface of the Al film and heated at 60℃ for 24 h. Finally, the obtained electrode film was used as cathode. The lithium film was used as anode and counter electrode. The separator is clegard 2300.

The constant discharge and charge profiles were obtained on the LANDCT2001A with the voltage between 1.5 and 3.0 V. Electrochemical impedance spectra was tested by using the electrochemistry station (CHI660E).

3. RESULTS AND DISCUSSION

Figure 1 shows the schematic illustration for the preparation of the S/$NiCo_2O_4$ composite. As shown in Figure 1, the pristine $NiCo_2O_4$ nanofibers are firstly prepared by using electrospinning method. This step could ensure the morphology of the $NiCo_2O_4$. Because the electrospinning method is beneficial for preparing hollow nanofibers structure materials. The 3D nanofibers structure could accelerate the transportation of the electronics, resulting superior electronic conductivity. Then, the pristine $NiCo_2O_4$ was calcined at 500 ℃ for 2 h to obtain the hollow structure $NiCo_2O_4$. Finally, the mixture of $NiCo_2O_4$ and sulfur was heated at 155 ℃ for 12 h to prepare the S/$NiCo_2O_4$ composites. At the temperature of 155 ℃, the element sulfur achieves the optimal viscosity. As a result, the element sulfur could easily immerse into the hollow nanofiber structure of $NiCo_2O_4$.

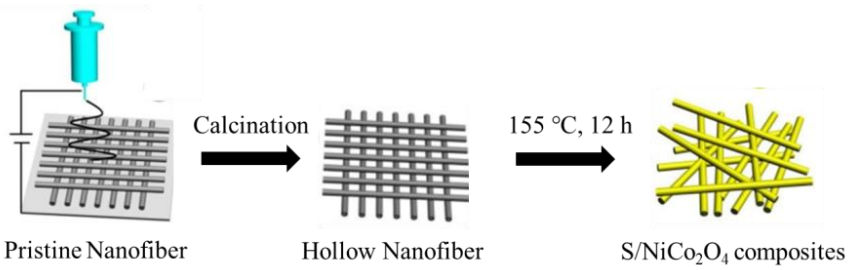

Figure 1. Schematic illustration for the preparation of the S/$NiCo_2O_4$ composite.

Figure 2a and b exhibit the SEM images of the hollow $NiCo_2O_4$ nanofiber and S/$NiCo_2O_4$ composites. As shown in Figure 2a, the $NiCo_2O_4$ shows hollow nanofiber structure with dimeter of 10 nm. The hollow nanofiber structure could be easily observed from the SEM image. This hollow structure provides sufficient space for the storage of the element sulfur. For the S/$NiCo_2O_4$ composites, it displays similar structure compared with the pure $NiCo_2O_4$ nanofiber. Especially, the surface of the S/$NiCo_2O_4$ composite becomes smooth [17]. This may be ascribed to the presence of element sulfur on the surface of the hollow $NiCo_2O_4$ nanofiber. Furthermore, Figure 2c and d is the TEM images. It can be seen that after heating with the sulfur, the TEM image has no obvious change, indicating that the element sulfur is uniformly immersed into the hollow structure of $NiCo_2O_4$.

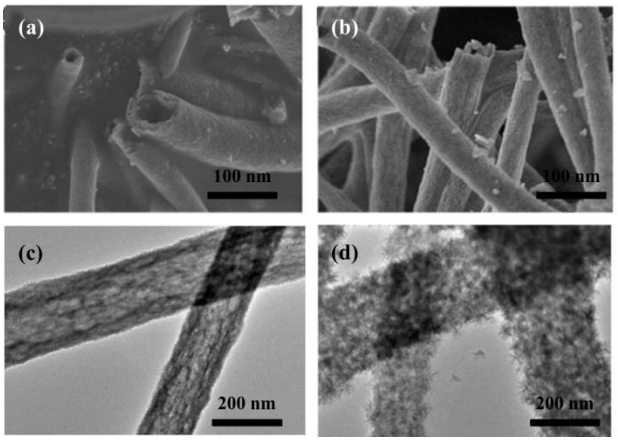

Figure 2. SEM image of (a) S/$NiCo_2O_4$ composites, TEM image of (b) S/$NiCo_2O_4$ composites.

Figure 3a is the XRD pattern of the $NiCo_2O_4$ and S/$NiCo_2O_4$ composites. As shown in Figure 3a, the as-prepared $NiCo_2O_4$ displays typical crystal structure. Besides, it is matched well with the standard card (JCPDS 73-1702), confirming the high purity of the $NiCo_2O_4$ [18]. The S/$NiCo_2O_4$ composites show many diffraction peaks of element sulfur, indicating the successful preparation of the S/$NiCo_2O_4$ composites. The high purity of the samples could ensure the superior electrochemical performance. To investigate the chemical environment of various elements, XPS was conducted for the S/$NiCo_2O_4$ composites.

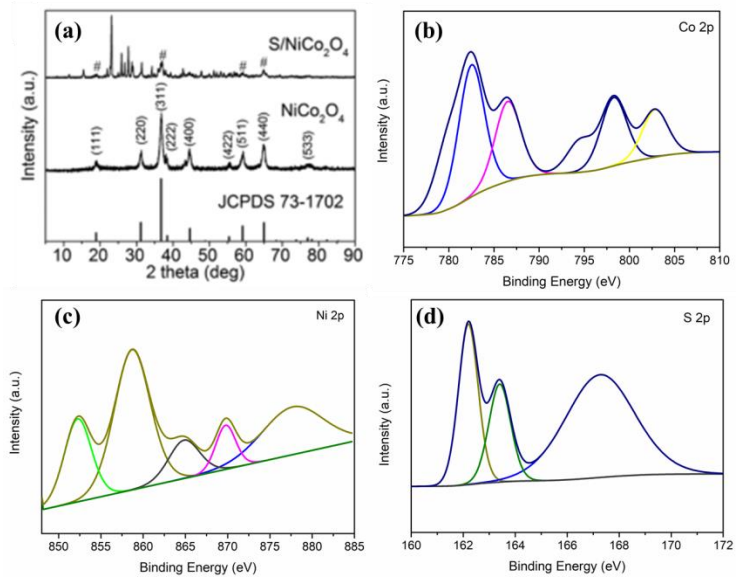

Figure 3. (a) The XRD pattern of the S/$NiCo_2O_4$ composites. XPS of (b) Co 2p, (c) Ni 2p and (d) S 2p for the S/ $NiCo_2O_4$ composites.

For the Co 2p (Figure 3b), the peaks at 781.6 eV and 796.5 eV are related to the Co $2p_{3/2}$ and Co $2p_{1/2}$. In terms of the Ni 2p (Figure 3c), it can be seen that there are two main peaks at 856.8 eV and 880.2 eV [19]. They are corresponding to the Ni $2p_{3/2}$ and Ni $2p_{1/2}$. Moreover, the peak at 870.2 eV is

the satellite front [20]. The peak at 865.8 eV may contribute to the presence of the Ni-S bond. For the S 2p (Figure 3d), the peaks at 162.8 eV and 168.0 eV represent the S $2p_{3/2}$ and S $2p_{1/2}$ [21], respectively. Therefore, it can be observed that there is Ni-S bond in the S/$NiCo_2O_4$ composites. Many works have reported that the chemical adsorption has strong adsorbent ability for the polysulfide. This chemical bond is beneficial for adsorbing the polysulfide in the electrolyte. Moreover, the chemical adsorption for the soluble polysulfide is much stronger than the traditional physical sorption.

Figure 4a is the constant DC curves of the as-prepared S/$NiCo_2O_4$ electrode at the current density of 0.2 C. The initial specific capacity of the S/$NiCo_2O_4$ electrode is as high as 1096 mAh g^{-1}. In all, there are two voltage platforms in the discharge profile at 2.3 V and 2.1 V, respectively. This is consistent with the CV curves (Figure 5). Figure 4b shows the DC curves of the S/$NiCo_2O_4$ electrode at various sulfur loadings from 3 mg cm^{-2} to 4 mg cm^{-2}. It can be seen that the specific capacity values are 896 mAh g^{-1} and 892 mAh g^{-1} at the sulfur loadings of 2 mg cm^{-2} and 3 mg cm^{-2}, respectively. Even at the sulfur loading of 4 mg cm^{-2}, the specific capacity is still at 835 mAh g^{-1}, which is higher than many reported cathode materials. This is attributed to the hollow nanofiber structure, which is beneficial for the transportation of electronics and lithium-ions. As a result, the electronic conductivity of the whole cathode is greatly improved.

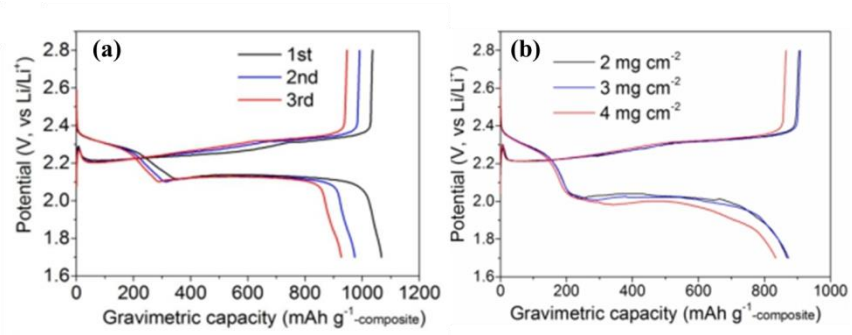

Figure 4. (a) The 1st, 2nd and 3rd discharge and charge profiles of the S/$NiCo_2O_4$ electrode at the current density of 0.2 C. (b) The DC curves of the S/$NiCo_2O_4$ electrode at the current density of 1 C with various sulfur loading from 2 mg cm^{-2} to 4 mg cm^{-2}.

CV curves are used to judge the electrochemical reaction in the electrode materials. As shown in Figure 5, the CV curves consists two reduction peaks at 2.3 V and 2.0 V, respectively. They are corresponding to the element sulfur to soluble polysulfide and polysulfide to Li_2S. Besides, there are two oxidation peaks at 2.4 V and 2.3 V, which are related to the inverse transformation. Moreover, it can be seen that the CV curves overlap well from the 2nd cycles, demonstrating superior electrochemical reversibility. With the increase of the cycle numbers, the CV curves show excellent electrochemical reversibility.

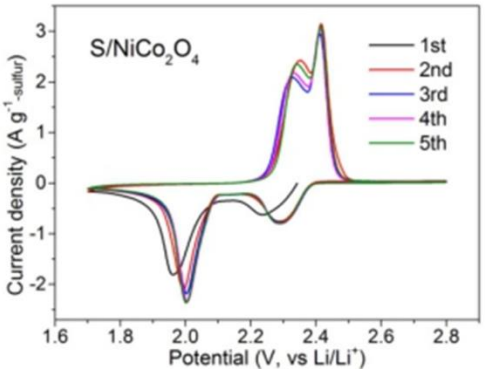

Figure 5. The CV curves of the S/$NiCo_2O_4$ electrode.

Figure 6 shows the cycle performance of the S/$NiCo_2O_4$ electrode with high-loading sulfur of 4 mg cm^{-2}. The as-prepared S/$NiCo_2O_4$ composites exhibit excellent cycle stability with capacity retention of 78% after 100 cycles even at the current density of 1C. As we all know, the cycle performance becomes bad with the increase of the sulfur loading. The sulfur loading is under 2 mg cm^{-2} in many reported works. Therefore, the as-prepared S/$NiCo_2O_4$ composites show superior cycle stability with high sulfur loading, which is related to the employment of the $NiCo_2O_4$. The presence of the $NiCo_2O_4$ could provide chemical absorption for the soluble polysulfide and inhibit the shuttle effect of the polysulfide from the cathode to the anode. In fact, the electrochemical performance became bad with the increase of the sulfur loading in the lithium-sulfur battery. The great amount sulfur will consume the electrolyte. Moreover, the sufficient polysulfide dissolved into the electrolyte, causing the increase of the viscosity.

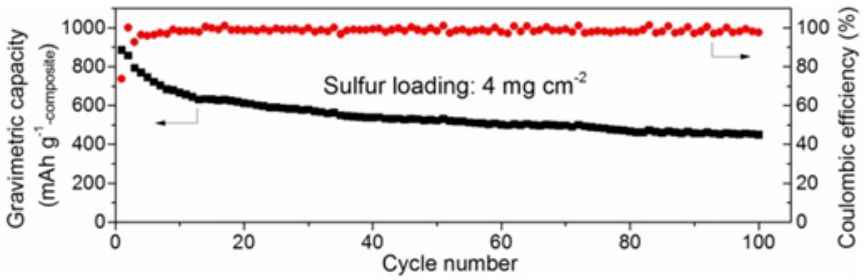

Figure 6. The cycle stability of the S/$NiCo_2O_4$ electrode at the current density of 1 C for 100 cycles.

To further demonstrate the superior cycle stability of the S/$NiCo_2O_4$ cathode materials, a table was made to compare their electrochemical performances. As shown in Table 1, it can be seen that the as-prepared S/$NiCo_2O_4$ cathode has high sulfur loading with 4 mg cm^{-2}, showing superior cycle stability at 1 C at the same time. While other reported cathode materials display rapid capacity fading at low sulfur loading condition. Therefore, the employment of S/$NiCo_2O_4$ cathode materials is beneficial for the improvement of the cycle stability of the lithium-sulfur batteries.

Table 1. Electrochemical performances of various cathode materials for Li-S batteries.

Electrode	Current Density	Sulfur Loading	Capacity	Ref
S@pPAN	1 C	3 mg cm^{-2}	439 mAh g^{-1}	22
NiS_2/rGO/S	1 C	1.5 mg cm^{-2}	510 mAh g^{-1}	23
Fe_3O_4@C	1 C	2 mg cm^{-2}	487 mAh g^{-1}	24
S/$NiCo_2O_4$	1 C	4 mg cm^{-2}	526 mAh g^{-1}	This Work

To confirm the inhibition of the soluble polysulfide from the cathode side to the anode side, the SEM and EDS of the lithium anode were tested after 100 cycles. As shown in Figure 7 a and b, the element sulfur could hardly be observed at the surface of the lithium anode, which is faced with the S/$NiCo_2O_4$ cathode [25]. However, for the pure sulfur cathode (Figure 7 c and d), it can be seen that many element sulfur particles are located on the surface of the lithium anode. This is ascribed to the shuttle effect of the polysulfide from the cathode side to the anode lithium side. From this result, it can be concluded that the employment of the S/$NiCo_2O_4$ cathode is beneficial for the inhibition of the shuttle effect of the polysulfide from the cathode to the lithium anode side [26].

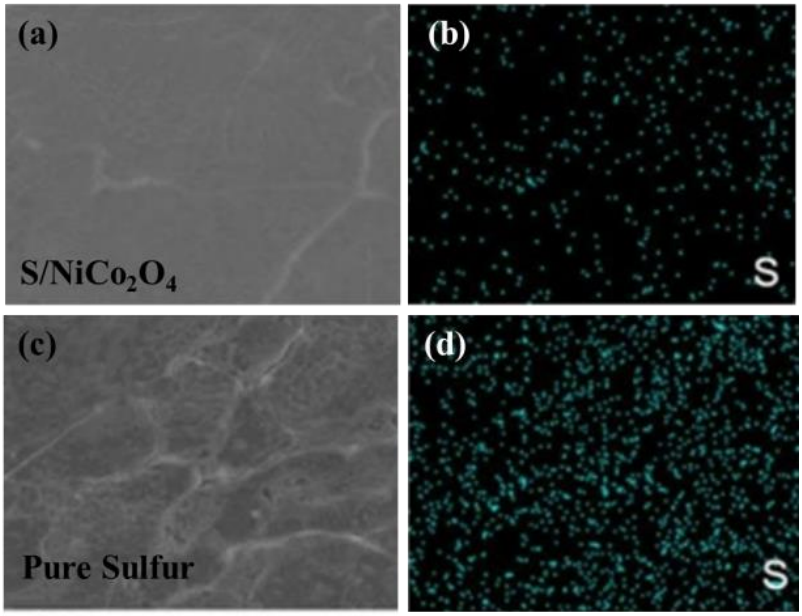

Figure 7. SEM images and the corresponding EDS of Li anode for (a), (b) S/$NiCo_2O_4$ cathode and (c), (d) pure sulfur cathode after 100 electrochemical cycles.

4. CONCLUSIONS

In summary, the high-loading sulfur lithium-sulfur battery is prepared via using hollow $NiCo_2O_4$ nanofibers as the host materials for the element sulfur. The electrochemical results show that

the as-prepared S/$NiCo_2O_4$ electrode exhibits high specific capacity value of 1096 mAh g^{-1} at the current density of 0.2 C. Moreover, the specific capacity of the as-prepared S/$NiCo_2O_4$ electrode is as high as 526 mAh g^{-1} with the sulfur loading of 4 mg cm^{-2} after 100 cycles at the current density of 1 C. As a result, our work may provide a promising method for preparing the high-loading sulfur lithium-sulfur battery.

ACKNOWLEDGEMENT
This study was supported by Key Scientific and Technological Research Projects in Henan Province (192102210028), the National Natural Science Foundation of China (51602358) and the Education Department of Henan Province Natural Science Research Program (18B150029).

References

1. L. L. Fan, N. P. Deng, J. Yan, Z. H. Li, W. M. Kang and B. W. Cheng, *Chem. Eng. J*., 369 (2019) 874.
2. L. L. Fan, M. Li, X. F. Li, W. Xiao, Z. W. Chen and J. Lu, *Joule*, 3 (2019) 361.
3. Q. Zhang, X. F. Zhang, M. Li, J. Q. Liu and Y. C. Wu, *Appl. Surf. Sci*., 487 (2019) 452.
4. L. Zhang, B. Wu, Q. F. Li and J. F. Li, *Appl. Surf. Sci*., 484 (2019) 1184.
5. J. Wu, S. Y. Li, P. Yang, H. P. Zhang, C. Du, J. M. Xu and K. X. Song, *J. Alloy Compd*., 783 (2019) 279.
6. S. K. Lee, Y. J. Lee and Y. K. Sun, *J. Power Sources*, 323 (2016) 174.
7. X. C. Gao, Y. J. Shen, L. L. Xing, Q. Wang and X. Y. Xue, *Mater. Lett*., 183 (2016) 413.
8. T. B. Zeng, X. B. Hu, P. H. Ji and G. P. Zhou, *Solid State Ionics*, 291 (2016) 47.
9. W. Yang, W. Yang, J. N. Feng, Z. P. Ma and G. J. Shao, *Electrochim. Acta*, 210 (2016) 71.
10. Z. G Yao, S. P. Wang, K. Dong, Y. Dai and X. R. Lei, *Electrochim. Acta*, 187 (2016) 629.
11. Z. H. Li, X. G. Li,, Y. H. Liao, X. P. Li and W. S. Li, J. Power Sources, 334 (2016) 23.
12. J. Y. Lee, S. K. Park and Y. Z. Piao, *Electrochim. Acta*, 222 (2016) 1345.
13. H. H. Xu, L. Qie and A. Manthiram, *Nano Energ*., 26 (2016) 224.
14. K. Ding, Q. Liu, Y. K. Bu, K. Meng, W. J. Wang, D. Q. Yuan and Y. B. Wang, *J. Alloy Compd*., 657 (2016) 626.
15. Z. L. Peng, R. G. Li, J. D. Gao, Z. X. Yang, Z. H. Deng and J. S. Suo, *Electrochim. Acta*, 220 (2016) 130.
16. S. D. Seo, C. H. Choi and D. W. Kim, *Mater. Lett*., 172 (2016) 116.
17. L. Zhang, B. Wu, Q. F. Li and J. F. Li, *Appl. Surf. Sci*., 484 (2019) 1184.
18. X. L. Lu, Q. F. Zhang, J. Wang, S. H. Chen and B. G. Lu, *Chem. Eng. J*., 358 (2019) 955.
19. S. Y. Majumder, M. H. Shao, Y. F. Deng and G. H. Chen, 431 (2019) 93.
20. J. Wu, S. Y. Li, P. Yang, H. P. Zhang, C. Du, J. M. Xu and K. X. Sun, *J. Alloy Compd*., 783 (2019) 279.
21. Y. D. Li, Q. Wang, D. G. Zheng, W. P. Li and J. X. Wang, *J. Alloy Compd*., 787 (2019) 982.
22. S. P. Li, Z. L. Han, W. Hu, L. F. Peng, J. Q. Yang, L. H. Wang, Y. Y. Zhang, B. Shan and J. Xie, *Nano Energ*., 60 (2019) 153.
23. Y. Li, J. Chen, Y. F. Zhang, Z. Y. Yu, T. Z. Zhang, W. Q. Ge and L. P. Zhang, *J. Alloy Compd*., 766 (2018) 804.
24. G. X. Liu, K. Feng, H. T. Cui, J. Li, Y. Y. Liu and M. R. Wang, *Chem. Eng. J*., 381 (2020) 122652.
25. Q. Zhang, S. Bolisetty, Y. Cao, S. Handschin, J. Adamcik, Q. Pengand R. Mezzenga, *Angew. Chem.*

Int. Edit., 58 (2019), 6012.
26. N. Li, S. F. Tang, Y. D. Rao, J. B. Qi, Q. R. Zhang, D. L. Yuan, *Electrochim. Acta* 298 (2019) 59.